AJNR

In Vivo Imaging of Venous Side Cerebral Small-Vessel Disease in Older Adults: An MRI Method at 7T

C.E. Shaaban, H.J. Aizenstein, D.R. Jorgensen, R.L. MacCloud, N.A. Meckes, K.I. Erickson, N.W. Glynn, J. Mettenburg, J. Guralnik, A.B. Newman, T.S. Ibrahim, P.J. Laurienti, A.N. Vallejo and C. Rosano

AJNR Am J Neuroradiol 2017, 38 (10) 1923-1928
doi: https://doi.org/10.3174/ajnr.A5327
http://www.ajnr.org/content/38/10/1923

In Vivo Imaging of Venous Side Cerebral Small-Vessel Disease in Older Adults: An MRI Method at 7T

C.E. Shaaban, H.J. Aizenstein, D.R. Jorgensen, R.L. MacCloud, N.A. Meckes, K.I. Erickson, N.W. Glynn, J. Mettenburg, J. Guralnik, A.B. Newman, T.S. Ibrahim, P.J. Laurienti, A.N. Vallejo, and C. Rosano, for the LIFE Study Group

ABSTRACT

BACKGROUND AND PURPOSE: Traditional neuroimaging markers of small-vessel disease focus on late-stage changes. We aimed to adapt a method of venular assessment at 7T for use in older adults. We hypothesized that poorer venular morphologic characteristics would be related to other small-vessel disease neuroimaging markers and a higher prevalence of small-vessel disease–Alzheimer disease risk factors.

MATERIALS AND METHODS: Venules were identified in periventricular ROIs on SWI and defined as tortuous or straight. The tortuosity ratio was defined as total tortuous venular length divided by total straight venular length. White matter hyperintensity burden (visually rated from 0 to 3) and the number of microbleeds (0, 1, >1) were determined. Differences in tortuous and straight venular lengths were evaluated. Relationships with demographic variables, allele producing the e4 type of *apolipoprotein E* (*APOE4*), growth factors, pulse pressure, physical activity, and Modified Mini-Mental State Examination were assessed via Spearman correlations.

RESULTS: Participants had 42% more tortuous venular tissue than straight (median, 1.42; 95% CI, 1.13–1.62). *APOE4* presence was associated with a greater tortuosity ratio ($\rho = 0.454$, $P = .001$), and these results were robust to adjustment for confounders and multiple comparisons. Associations of the tortuosity ratio with sex and vascular endothelial growth factor did not survive adjustment. Associations of the tortuosity ratio with other variables of interest were not significant.

CONCLUSIONS: Morphologic measures of venules at 7T could be useful biomarkers of the early stages of small-vessel disease and Alzheimer disease. Longitudinal studies should examine the impact of *apolipoprotein E* and vascular endothelial growth factor on the risk of venular damage.

ABBREVIATIONS: AD = Alzheimer disease; *APOE4* = allele producing the e4 type of *apolipoprotein E*; BDNF = brain-derived neurotrophic factor; IQR = interquartile range; LIFE MRI = Lifestyle Interventions and Independence for Elders Magnetic Resonance Imaging study; 3MS = Modified Mini-Mental State Examination; SVD = small-vessel disease; VEGF = vascular endothelial growth factor; WMH = white matter hyperintensities

Cerebral small-vessel disease (SVD) increases dementia risk[1] and vulnerability to Alzheimer disease (AD) neuropathology.[2] Neuroimaging methods investigating SVD have traditionally relied on WM hyperintensities (WMHs). However, WMH is a marker of late-stage SVD, reflecting advanced parenchymal damage, reduced CBF, and abnormalities of the small penetrating vessels.[3] Thus, there is a need for radiologic markers that capture the earlier stages of SVD relating directly to vessel health.

With aging and hypertension, arteries have a reduced ability to absorb flow pulsatility, thus transmitting highly pulsatile flow to the venules. Venular walls are well-equipped to handle low pulsatile and slow flow, but not highly pulsatile flow. Pulsatility-related damage can induce venular morphologic changes such as collagenosis, leading to loss of elasticity and lumen narrowing/occlusion, which, in turn, promote ischemia. Both collagenosis and

Received October 25, 2016; accepted after revision May 28, 2017.

From the Graduate School of Public Health, Department of Epidemiology (C.E.S., D.R.J., N.W.G., A.B.N., C.R.), Center for the Neural Basis of Cognition (C.E.S., H.J.A., D.R.J., K.I.E., C.R.), Departments of Psychiatry (H.J.A., R.L.M.), Biological Sciences (N.A.M.), Psychology (K.I.E.), Radiology (J.M., T.S.I.), Bioengineering (T.S.I.), and Immunology (A.N.V.). University of Pittsburgh, Pittsburgh, Pennsylvania; Department of Epidemiology and Public Health (J.G.), University of Maryland School of Medicine, Baltimore, Maryland; Laboratory for Complex Brain Networks (P.J.L.) and Department of Radiology (P.J.L.), Wake Forest University School of Medicine, Winston-Salem, North Carolina; and Department of Pediatrics (A.N.V.), Children's Hospital of Pittsburgh, Pittsburgh, Pennsylvania.

Research reported in this publication was supported by the National Institute on Aging under award Nos. U01 AG022376, F31 AG054084 (C.E.S.), R01 AG044474 (C.R.), and P30 AG024827. C.E.S. also received support from a training grant from the National Institute of General Medical Sciences under award No. T32 GM081760.

The content is solely the responsibility of the authors and does not necessarily represent the official views of the National Institutes of Health.

Please address correspondence to Caterina Rosano, MD, MPH, Department of Epidemiology, Graduate School of Public Health, University of Pittsburgh, 130 DeSoto St, 5139 Parran South, Pittsburgh, PA 15261; e-mail: rosanoc@edc.pitt.edu

Indicates open access to non-subscribers at www.ajnr.org
Indicates article with supplemental on-line appendix and table.
Indicates article with supplemental on-line photos.

http://dx.doi.org/10.3174/ajnr.A5327

tortuosity lead to reduced CBF and increased upstream resistance, exacerbating arterial pathology. Extravasation and inflammatory response, including focal perivascular parenchymal infiltration, can also occur, facilitated by the lack of tight junctions on the venous-side circulation.[4] Inflammatory cascades further damage the vasculature, reduce CBF, and compromise the BBB. These phenomena can become apparent as morphologic changes such as tortuosity, collagenosis, and thicker basal lamina. Such changes have been seen in vivo in AD[5] and in postmortem studies, and they appear more common with older age and in proximity to regions with WMHs.[6-8] Although the possibility has not been tested directly, venular morphologic alterations are considered to precede radiologically overt WMHs.

Ultra-high-field (7T) MR imaging has emerged as a noninvasive method to visualize venous microcirculation.[9,10] Specifically, SWI exploits the paramagnetic properties of deoxyhemoglobin to visualize venules without a contrast agent. Methods to quantify venules in multiple sclerosis,[11] sickle cell anemia,[12] CADASIL,[7,13] and, recently, AD[14] have been reported. However, venular characteristics in relation to cerebral SVD in aging are unknown.

Our primary aim was to demonstrate the feasibility of adapting published methods[11,12] to study venular characteristics in older adults. Our secondary aim was to evaluate the relationships of venular characteristics with neuroimaging markers of SVD—WMH and microbleeds—and variables relevant to SVD and AD. We hypothesized that poorer venular morphologic characteristics would be related to other SVD neuroimaging markers and a higher prevalence of SVD-AD risk factors.

MATERIALS AND METHODS

Participants

The Lifestyle Interventions and Independence for Elders Magnetic Resonance Imaging study (LIFE MRI) is a neuroimaging study within a randomized controlled trial, which demonstrated that physical activity prevents major mobility disability in at-risk community-dwelling older adults versus health education control (hazard ratio, 0.82, $P = .03$).[15] The study protocol was approved by the University of Pittsburgh institutional review board. All participants provided written informed consent. The present study ($n = 53$) used images from the baseline visit.

The LIFE study design has been previously reported.[16] The On-line Table shows inclusion/exclusion criteria. Participants were not screened for MR imaging on the basis of caffeine use due to minimal reported average caffeine-related signal change of veins in white matter ($-2 \pm 1.2\%$).[17] On-line Fig 1 shows participant flow.

Sample Characteristics

Age, race, and sex, self-reported by participants, were evaluated because of their association with SVD and AD.[18-22] *Apolipoprotein E* was genotyped by using TaqMan (TaqMan probe C__904973_10; Applied Biosystems, Life Technologies, Foster City, California) and pyrosequencing.[23] The allele producing the e4 type of *apolipoprotein E* (*APOE4*) is the strongest genetic risk factor for late-onset AD.[24] Pulse pressure (systolic blood pressure–diastolic blood pressure; average of 2-seated measurements) and physical activity were assessed because of their associations with AD[25,26] and SVD.[27,28] Physical activity was measured for 7 days by using hip-worn accelerometry (GT3X; Actigraph, Pensacola, Florida) as minutes per day of moderate physical activity. Finally, the Modified Mini-Mental State Examination (3MS)[29] was included as a measure of global cognition.

Growth Factors

The angiogenic factors vascular endothelial growth factor (VEGF)[30] and brain-derived neurotrophic factor (BDNF)[31] were measured via the Luminex system with kits (Human Cancer Panel and Neurodegenerative Disease Panel; EMD Millipore, Hercules, California). Fasting blood, collected by venipuncture, remained at room temperature for 30–60 minutes to clot and was then centrifuged at 1600 x g for 15 minutes at 4°C. Serum was aliquoted and immediately frozen at −70°C or lower and stored until analysis. Concentrations were determined with 2 sets of standard curves, with final values calculated according to standardized procedures we have validated.[32]

Potential Confounders

Self-reported antihypertensive medication use, which may affect pulse pressure, was recorded. Blood hemoglobin level was measured because it may affect venular conspicuity on SWI. We also recorded SWI voxel size, which varied among the participants.

Outcome Variables

Venular Characteristics. Axial susceptibility-weighted MRIs were obtained at the University of Pittsburgh MR Research Center by using a Rapid Biomedical (Rimpar, Germany) 8-channel head coil on a Siemens (Erlangen, Germany) 7T scanner (TR = 2000 ms, TE = 15 ms), acquired with $0.25 \times 0.25 \times 1.50$ mm ($n = 40$), $0.23 \times 0.23 \times 3.00$ mm voxels, interleave gap = 0.60 mm ($n = 12$), or with $0.50 \times 0.50 \times 1.00$ mm voxels ($n = 5$). When necessary, scans were resampled to 1.50-mm section thickness.

A 4×1 cm ROI was placed in each hemisphere, 1 section below the uppermost section on which ventricular CSF was visible. To maintain consistency, we placed the ROI on the basis of native-space landmarks, centered along the anteroposterior length of the ventricle, and on the lateral wall of the ventricle (On-line Fig 2). The ROI was chosen because it corresponds to regions known to be vulnerable to SVD,[5,13,14] is consistent with published methods,[11,12] and allows the greatest consistency in vessel orientation, with a clear course perpendicular to the length of the lateral ventricles. The minimum intensity projection was applied over 3 sections (4.5 mm) to improve visualization.[9]

Three raters (C.E.S., D.R.J., N.A.M.) were trained and overseen by a certified neuroradiologist (J.M.) and the study Principal Investigator (C.R.). First, published protocols were studied and discussed among the raters, neuroradiologist, Principal Investigator, and coinvestigators (H.J.A., R.L.M.). Next, the same 5 MRIs were rated by the raters, each blinded to the tracings of the other 2 raters. Last, each venular tracing was discussed among the raters and with the neuroradiologist and Principal Investigator regarding the presence/absence of the venule and straight/tortuous course. This discussion continued until the raters were proficient in tracing and the results of their consensus were consistent with the judgment of the neuroradiologist/Principal Investigator.

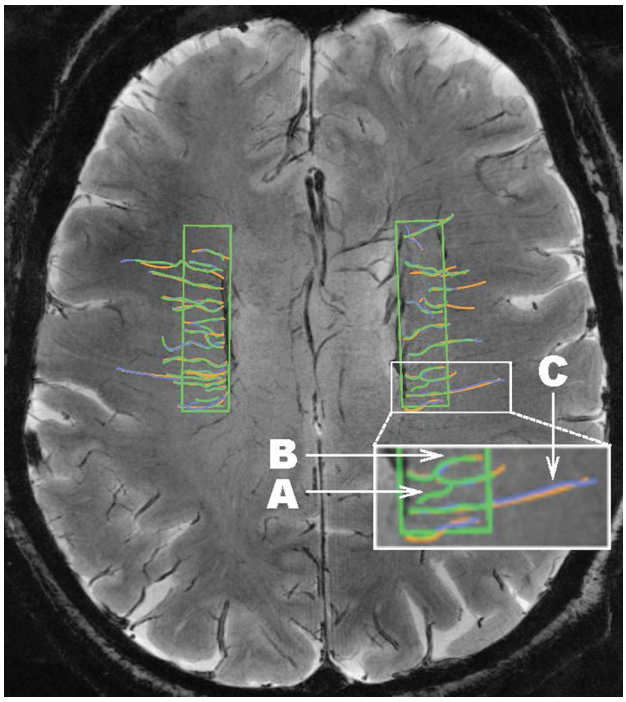

FIG 1. A sample consensus venular tracing on SWI at 7T across ROIs in both hemispheres in the LIFE MRI study. Each rater traces the venules. A different color (green, purple, orange) is assigned to each rater, and the 3 sets of tracings are then overlaid. Inset in white is shown at larger magnification at the bottom of the figure to illustrate: *A*, An example of a venule that would not be included in the dataset because it was traced by only 1 of the 3 raters (green). *B*, An example of a tortuous venule. *C*, An example of a straight venule.

Tracing was done with OsiriX Imaging Software (http://www.osirix-viewer.com).[33] Criteria to identify a venule were the following: a linear structure of intensity darker than the surrounding parenchyma; length, ≥3 mm; and coursing through the ROI for ≥3 mm (to reduce interrater variability of inclusion for vessels along the edge of the ROI). Most venules could be followed to obvious deep veins, and the dark appearance and orientation axial to the ventricles and deep within the white matter also helped to identify the origin of the vessels as venous. Venules were traced across their full length, even if they continued outside the ROI, to avoid artificial truncation. After all venules were traced, the presence/absence of a venule was adjudicated by consensus among raters. A venule was included only if ≥2 of the 3 raters had traced it (Fig 1). Next, the venular course (straight/tortuous) was rated during the consensus meeting. A vessel that ran free of inflection points ≥30° for most of its total length (>60%) was defined "straight"; otherwise the vessel was defined "tortuous." The length of each venule was computed as the median value of the lengths measured by the raters tracing that venule. The number and length of all consensus-traced venules were summed, and total and average lengths (total length/venule number) were obtained for each participant.

Tortuous venules are present in areas with WMHs[6]; thus, we evaluated tortuous and straight venules separately. The tortuosity ratio was calculated as the total tortuous length divided by the total straight length. Thus, a tortuosity ratio of >1 indicates greater tortuous venular length than straight length. Due to blood oxygen level–dependent–related signal blooming, measures of diameter may not have been accurate; thus, we did not quantify diameter.

White Matter Hyperintensities. WMH was imaged with T2WI (TR = 12,500 ms, TE = 55 ms, voxel size = 0.5 × 0.5 × 6.0 mm) and MPRAGE (TR = 3430 ms, TE = 3.54 ms, voxel size = 0.7 mm^3 isotropic) and was rated by a consensus of 2 raters (C.R., H.J.A.) with a 0–3 modified Fazekas rating scale.[34] Ratings consisted of the following: 0 = none: no punctate hyperintense areas or periventricular rims; 1 = mild: few punctate hyperintense areas and/or limited amount of hyperintense rims around the ventricular horns; 2 = moderate: multiple punctate hyperintense areas and/or larger rims around the ventricular horns; or 3 = severe: confluent subcortical hyperintense areas and/or rims all around the ventricles, including the horns and sides. Only 4/53 had no WMHs (WMH = 0), leaving 92% with at least mild WMHs; thus, we combined 0 and 1 to create a "none/mild" category. Because the distinction between periventricular and deep WMHs is not consistently meaningful, we did not differentiate them.[35]

Microbleeds. We classified cerebral microbleeds on the basis of Greenberg et al.[36] Two trained raters (N.A.M., E.L.T.) characterized microbleeds under the supervision of a neuroradiologist (J.M.). Microbleeds were defined as black or substantially hypointense on SWI, round or ovoid (confirmed on adjacent sections), and at least half surrounded by brain parenchyma. To take advantage of the ability of the 7T magnet to capture quite small microbleeds, we did not use a minimum size criterion. Final ratings were based on consensus, with disagreements mediated by the neuroradiologist. We counted the total number of microbleeds across all 64 sections of the axial SWI and categorized totals as 0, 1, or >1 microbleed.

Statistical Analysis

Descriptive statistics were calculated as counts and percentages, means and SDs, or medians and interquartile ranges (IQRs). Differences were tested with *t* tests, Wilcoxon rank sum tests, or χ^2 tests, $\alpha = .05$. We also determined the median tortuosity ratio and calculated the 95% CIs by using 10,000 bootstrapped samples.

We explored the relationships of the tortuosity ratio with other neuroimaging markers of SVD, including WMH and microbleeds; nonmodifiable factors, including demographic variables (age, race, and sex), and *APOE4*; potentially modifiable factors, including growth factors (VEGF and BDNF), pulse pressure (adjusted for antihypertensive medication use), and physical activity; 3MS; and hemoglobin, with Spearman correlations, $\alpha = .10$. Significant correlations with the tortuosity ratio were re-evaluated as partial correlations adjusted for hemoglobin and voxel size. A false discovery rate of 0.10 was used to correct for multiple comparisons.

Statistical analysis was performed in SAS, Version 9.4[37] and SPSS version 22.[38]

RESULTS

MR imaging study participants were younger and less likely to be non-Hispanic white than the non-MR imaging study participants (Table 1). Of MR imaging study participants, 15/47 with *APOE* data had at least 1 copy of the *APOE4* allele. Thus, representation

Table 1: Study sample characteristics in the LIFE study at the Pittsburgh site

	MRI Study (n = 53)	Non-MRI Study (n = 163)	P Value
Age (median) (IQR) (yr)	76.0 (5.8)	79.4 (9.0)	<.01[a]
Race, non-Hispanic white (No.) (%)	30 (56.6)	124 (76.1)	<.01[a]
Sex, female (No.) (%)	42 (79.2)	123 (75.5)	.57
APOE4 allele presence[b] (No.) (%)	15 (31.9)	27 (20.0)	.10
VEGF (median) (IQR) (pg/mL)	414.61 (370.17)	–	
BDNF (median) (IQR) (pg/mL)	19,780.30 (27,492.00)	–	
Pulse pressure (median) (IQR)	53 (13)	57 (18)	.06
Physical activity—daily moderate activity (median) (IQR) (min)	24.6 (31.6)	18.3 (22.7)	.05
3MS (median) (IQR)	93 (7)	92 (9)	.46
Severe WMH burden[c] (No.) (%)	11 (20.8)	–	
No microbleeds[d] (No.) (%)	21 (39.6)	–	
Confounders			
On antihypertensive medication (No.) (%)	39 (73.6)	119 (73.0)	.93
Hemoglobin level[e] (median) (IQR) (g/dL)	12.7 (1.2)	13.2 (2.0)	.22

[a] Significant.
[b] Available on n = 47 (MRI) and n = 135 (non-MRI).
[c] WMH: rated as 0 = none/mild, 1 = moderate, 2 = severe.
[d] Available on n = 45 due to scan quality or motion; the remaining 24 were split nearly evenly between 1 and >1.
[e] Available on n = 47 (MRI) and n = 139 (non-MRI).

Table 2: Venular length measures in LIFE MRI (n = 53) for tortuous and straight venules separately

	Tortuous	Straight	P Value[a]
Total length of venules (mean) (SD) (mm)[c]	156.87 (53.18)	111.41 (50.11)	<.001[b]
No. of venules (mean) (SD)	18.09 (5.87)	13.11 (5.34)	<.001[b]
Average length of venules (mean) (SD) (mm)	8.64 (0.87)	8.30 (1.42)	.07

[a] P values based on paired t tests comparing tortuous and straight venule characteristics.
[b] Significant.
[c] Venule lengths: for each participant, venules were traced in 4-cm^2 ROIs (1 in each hemisphere), their length was measured by 3 raters, and median length was computed for each vessel. Venules are characterized as straight or tortuous. The total straight and tortuous venular length in millimeters is calculated for each participant.

Table 3: Spearman correlations of tortuosity ratio with variables of interest to SVD and AD in LIFE MRI (n = 53)

	ρ	P Value
Age	−0.023	.87
Race	0.202	.15
Sex	−0.304	.03[a]
APOE4	0.454	.001[a]
Pulse pressure[b]	0.206	.14
VEGF	−0.236	.096[a]
BDNF	0.227	.11
Hemoglobin level	0.266	.07[a]
Physical activity—daily moderate activity (min)	−0.187	.20
3MS	0.199	.15

[a] Significant.
[b] Partial correlation of pulse pressure and tortuosity ratio adjusted for antihypertensive drug use.

of *APOE4* was higher than the 14% estimate among controls worldwide[39] but did not differ significantly from non-MR imaging participants. No or mild WMHs were seen in 58.5% of participants, while 20.8% each had moderate and severe WMHs. Regarding microbleeds, 39.6% of the sample had 0, 20.8% had 1, and 24.5% had >1.

The total length of tortuous vessels ranged from 26.25 to 246.36 mm, while the total straight length ranged from 16.72 to 217.65 mm. The overall length of tortuous venules was greater than that of straight venules (Table 2). Total tortuous length was 42% greater than total straight length (median tortuosity ratio, 1.4; 95% bootstrapped CI, 1.13–1.62) (On-line Fig 3). To examine whether this finding was due to number of venules or average length, we evaluated differences in those measures. The total number of tortuous venules ranged from 4 to 32, while total straight venules ranged from 2 to 24. There were more tortuous venules than straight ones. The range of average tortuous length was 6.56–10.93 mm, while the range of average straight length was 4.35–11.57 mm, and these average lengths were not significantly different. Thus, the difference in total tortuous and straight venular lengths was driven by a greater number of tortuous venules.

Correlations between neuroimaging markers of SVD and the tortuosity ratio were not significant. WMH correlated at $\rho = -0.125$, $P = .37$, and microbleeds correlated at $\rho = -0.059$, $P = .70$.

Among nonmodifiable variables associated with AD and SVD, sex was associated with the tortuosity ratio (Table 3). Males had a higher tortuosity ratio (median, 2.15; IQR, 0.98) than females (median, 1.31; IQR, 0.71). Those with at least 1 copy of the *APOE4* allele had a higher tortuosity ratio (median, 2.15; IQR, 1.78) than those without it (median, 1.21; IQR, 0.75). Associations with age and race were not significant ($P > .10$).

Among modifiable factors potentially influencing venular characteristics, a higher VEGF was associated with a lower tortuosity ratio. There were no significant associations with BDNF, pulse pressure (adjusted for antihypertensive use), physical activity, or 3MS score ($P > .10$). Results were similar when using a ratio of vessel counts instead of the ratio of total lengths.

The relationship of *APOE4* with venular tortuosity, but not the other findings, remained significant after false discovery rate correction of the P value ($P = .01$). Further adjustment for hemoglobin level and voxel size did not modify the association with *APOE4*.

DISCUSSION

We found that application of 7T SWI is feasible to image cerebral venular characteristics in vivo in older adults. This method is a novel way of visualizing an understudied component of the cerebral vasculature. Given associations of venular tortuosity with SVD[6] and AD[40,41] as well as increases in microvascular changes with age,[8] venular tortuosity may serve as a marker of declining cerebrovascular integrity. This method may afford earlier detection of SVD and has the advantage of characterizing venular morphology without contrast.

We also found that *APOE4* was associated with a higher tortuosity ratio, and this association was robust to adjustment for potential confounders and multiple comparisons. This result supports studies implicating *APOE4* in reduced vascular integrity.

The APOE4 protein can directly damage the vasculature.[42] *APOE* is associated with neuroimaging manifestations of SVD,[43,44] and there are indications that it is associated with microvascular changes. Mice expressing transgenic human *APOE4* have altered basement membrane protein expression.[45] In humans with AD, *APOE4* is associated with BBB disruption.[46] *APOE4* is associated with both increased deposition and reduced clearance of β amyloid.[42] Clearly, *APOE4* is central to the development of AD pathology, and our results suggest it could be implicated in venular damage. It is possible that β amyloid deposition induces venular damage. An AD mouse model showed that as β amyloid built up in the arterioles beginning at 5 months of age, venular mural cells were damaged by 7 months of age.[41] However, it is also possible that venular damage induces β amyloid deposition. In this same experimental model, further venular mural cell damage led to increased arteriolar β amyloid deposition and, most interesting, induction of venular tortuosity.[41] The temporality of venular damage and β amyloid deposition remains an open question. We were unable to collect amyloid imaging. Hence, future multimodal neuroimaging studies need to evaluate the timing and relationship of β amyloid burden and venular tortuosity.

Although our result is remarkably consistent with the proposed *APOE4*-mediated reduction of vascular integrity,[42] our study cannot clarify the underlying mechanisms. This limitation notwithstanding, *APOE4* being associated with venular tortuosity indicates the potential for risk stratification as an intervention strategy. Thus, other factors should be evaluated to offset *APOE4*-related risk.

We found a nonsignificant association of the tortuosity ratio with WMHs and microbleeds, which could be due to a lack of sensitivity in our visual ratings or the small sample size. Future larger studies should evaluate associations of the tortuosity ratio with WMH volume, a more sensitive measure compared with visual ratings. Alternatively, this lack of association may indicate that the tortuosity ratio is capturing novel, early information regarding vascular integrity. Future work should examine the relationships of the tortuosity ratio with other SVD neuroimaging markers and related cognitive and mobility impairment and clarify the temporal order of venular damage and other SVD neuroimaging manifestations. We predict that venular damage comes before traditional neuroimaging markers of SVD.

Our study has several limitations. The sample was not selected to have a particularly low or high SVD burden. Future studies should compare venular tortuosity ratios in those 2 groups. Larger samples will be needed to confirm associations with sex and VEGF. The venular measures are also 2D and, therefore, do not account for venules running out of the plane. However, this bias is nondifferential across our sample. Finally, MR imaging participants were younger and had a higher proportion of nonwhites, indicating that this sample may differ from that in the general community-dwelling older adult population.

Despite these limitations, our study has notable strengths. We applied ultra-high-field neuroimaging with a higher SNR than typically used to visualize novel venular characteristics. This allows smaller sample sizes at ultra-high-fields than would be required at lower field strengths. Because this neuroimaging study was also within a randomized controlled trial, these participants were extremely well-characterized, allowing us to control for potential confounding factors.

CONCLUSIONS

SWI at 7T offers a noninvasive method to image markers of cerebral venular integrity and fills an important gap in knowledge. Morphologic measures of venules at 7T could be useful biomarkers of the early stages of SVD and AD. Risk and protective factors, especially those that are modifiable, for these pathophysiologic changes should be evaluated. Future longitudinal multimodal studies characterizing venular integrity at 7T are warranted.

For the full LIFE study investigator listing, see the On-line Appendix.

ACKNOWLEDGMENTS

The authors thank Erica Lynn Tamburo for neuroimaging assistance and Joshua Michel for implementing standardized Luminex assays.

Disclosures: C.E. Shaaban—*RELATED*: *Grant*: National Institute on Aging, *Comments*: F31 AG054084,* Howard J. Aizenstein—*RELATED*: *Grant*: National Institutes of Health*; *UNRELATED*: *Grants/Grants Pending*: National Institutes of Health*; *Travel/Accommodations/Meeting Expenses Unrelated to Activities Listed*: National Institutes of Health. Dana R. Jorgensen—*UNRELATED*: *Grant*: National Heart, Lung, and Blood Institute, *Comments*: T32 HL083825. Rebecca L. MacCloud—*RELATED*: *Grant*: National Institutes of Health.* Nancy W. Glynn—*RELATED*: *Grant*: National Institutes of Health, *Comments*: I was funded by the parent National Institutes of Health grant that recruited the participants for this work.* Tamer S. Ibrahim—*UNRELATED*: *Grants/Grants Pending*: National Institutes of Health, *Comments*: R01 grants.* Paul J. Laurienti—*RELATED*: *Grant*: National Institutes of Health.* Abbe N. Vallejo—*RELATED*: *Grant*: National Institutes of Health, *Comments*: P30 AG024827.* Caterina Rosano—*RELATED*: *Grant*: R01AG044474*; *Support for Travel to Meetings for the Study or Other Purposes*: R01AG044474.* *Money paid to the institution.

REFERENCES

1. Prins ND, van Dijk EJ, den Heijer T, et al. **Cerebral white matter lesions and the risk of dementia.** *Arch Neurol* 2004;61:1531–34 CrossRef Medline
2. Rosano C, Aizenstein HJ, Wu M, et al. **Focal atrophy and cerebrovascular disease increase dementia risk among cognitively normal older adults.** *J Neuroimaging* 2007;17:148–55 CrossRef Medline
3. Wardlaw JM, Valdés Hernández MC, Muñoz-Maniega S. **What are white matter hyperintensities made of? Relevance to vascular cognitive impairment.** *J Am Heart Assoc* 2015;4:001140 CrossRef Medline
4. Bechmann I, Galea I, Perry VH. **What is the blood-brain barrier (not)?** *Trends Immunol* 2007;28:5–11 CrossRef Medline
5. Bouvy WH, Kuijf HJ, Zwanenburg JJ, et al; Utrecht Vascular Cognitive Impairment (VCI) Study group. **Abnormalities of cerebral deep medullary veins on 7 Tesla MRI in amnestic mild cognitive impairment and early Alzheimer's disease: a pilot study.** *J Alzheimers Dis* 2017;57:705–10 CrossRef Medline
6. Fazekas F, Kleinert R, Offenbacher H, et al. **Pathologic correlates of incidental MRI white matter signal hyperintensities.** *Neurology* 1993;43:1683–89 CrossRef Medline
7. Pettersen JA, Keith J, Gao F, et al. **CADASIL accelerated by acute hypotension: arterial and venous contribution to leukoaraiosis.** *Neurology* 2017;88:1077–80 CrossRef Medline
8. Moody DM, Brown WR, Challa VR, et al. **Periventricular venous collagenosis: association with leukoaraiosis.** *Radiology* 1995;194:469–76 CrossRef Medline
9. Haacke EM, Mittal S, Wu Z, et al. **Susceptibility-weighted imaging: technical aspects and clinical applications, Part 1.** *AJNR Am J Neuroradiol* 2009;30:19–30 Medline
10. Mittal S, Wu Z, Neelavalli J, et al. **Susceptibility-weighted imaging:**

technical aspects and clinical applications, Part 2. *AJNR Am J Neuroradiol* 2009;30:232–52 Medline
11. Sinnecker T, Bozin I, Dorr J, et al. **Periventricular venous density in multiple sclerosis is inversely associated with T2 lesion count: a 7 Tesla MRI study.** *Mult Scler* 2013;19:316–25 CrossRef Medline
12. Novelli EM, Elizabeth Sarles C, Jay Aizenstein H, et al. **Brain venular pattern by 7T MRI correlates with memory and haemoglobin in sickle cell anaemia.** *Psychiatry Res* 2015;233:18–22 CrossRef Medline
13. De Guio F, Vignaud A, Ropele S, et al. **Loss of venous integrity in cerebral small vessel disease: a 7-T MRI study in Cerebral Autosomal-Dominant Arteriopathy with Subcortical Infarcts and Leukoencephalopathy (CADASIL).** *Stroke* 2014;45:2124–26 CrossRef Medline
14. Kuijf HJ, Bouvy WH, Zwanenburg JJ, et al. **Quantification of deep medullary veins at 7 T brain MRI.** *Eur Radiol* 2016;26:3412–18 CrossRef Medline
15. Pahor M, Guralnik JM, Ambrosius WT, et al; LIFE study investigators. **Effect of structured physical activity on prevention of major mobility disability in older adults: the LIFE study randomized clinical trial.** *JAMA* 2014;311:2387–96 CrossRef Medline
16. Fielding RA, Rejeski WJ, Blair S, et al; LIFE Research Group. **The Lifestyle Interventions and Independence for Elders Study: design and methods.** *J Gerontol A Biol Sci Med Sci* 2011;66:1226–37 CrossRef Medline
17. Sedlacik J, Helm K, Rauscher A, et al. **Investigations on the effect of caffeine on cerebral venous vessel contrast by using susceptibility-weighted imaging (SWI) at 1.5, 3 and 7 T.** *Neuroimage* 2008;40:11–18 CrossRef Medline
18. de Leeuw FE, de Groot JC, Achten E, et al. **Prevalence of cerebral white matter lesions in elderly people: a population based magnetic resonance imaging study—the Rotterdam Scan Study.** *J Neurol Neurosurg Psychiatry* 2001;70:9–14 CrossRef Medline
19. Gao S, Hendrie HC, Hall KS, et al. **The relationships between age, sex, and the incidence of dementia and Alzheimer disease: a meta-analysis.** *Arch Gen Psychiatry* 1998;55:809–15 CrossRef Medline
20. Liao D, Cooper L, Cai J, et al. **The prevalence and severity of white matter lesions, their relationship with age, ethnicity, gender, and cardiovascular disease risk factors: the ARIC Study.** *Neuroepidemiology* 1997;16:149–62 Medline
21. Lindsay J, Laurin D, Verreault R, et al. **Risk factors for Alzheimer's disease: a prospective analysis from the Canadian Study of Health and Aging.** *Am J Epidemiol* 2002;156:445–53 CrossRef Medline
22. Steenland K, Goldstein FC, Levey A, et al. **A meta-analysis of Alzheimer's disease incidence and prevalence comparing African-Americans and Caucasians.** *J Alzheimers Dis* 2015;50:71–76 CrossRef Medline
23. Cavallari LH, Langaee TY, Momary KM, et al. **Genetic and clinical predictors of warfarin dose requirements in African Americans.** *Clin Pharmacol Ther* 2010;87:459–64 CrossRef Medline
24. Bertram L, McQueen MB, Mullin K, et al. **Systematic meta-analyses of Alzheimer disease genetic association studies: the AlzGene database.** *Nat Genet* 2007;39:17–23 CrossRef Medline
25. Beydoun MA, Beydoun HA, Gamaldo AA, et al. **Epidemiologic studies of modifiable factors associated with cognition and dementia: systematic review and meta-analysis.** *BMC Public Health* 2014;14:643 CrossRef Medline
26. Qiu C, Winblad B, Viitanen M, et al. **Pulse pressure and risk of Alzheimer disease in persons aged 75 years and older: a community-based, longitudinal study.** *Stroke* 2003;34:594–99 CrossRef Medline
27. Mitchell GF, van Buchem MA, Sigurdsson S, et al. **Arterial stiffness, pressure and flow pulsatility and brain structure and function: the Age, Gene/Environment Susceptibility–Reykjavik study.** *Brain* 2011;134(pt 11):3398–407 CrossRef Medline
28. Torres ER, Strack EF, Fernandez CE, et al. **Physical activity and white matter hyperintensities: a systematic review of quantitative studies.** *Prev Med Rep* 2015;2:319–25 CrossRef Medline
29. Teng EL, Chui HC. **The Modified Mini-Mental State (3MS) examination.** *J Clin Psychiatry* 1987;48:314–18 Medline
30. Gerhardt H. **VEGF and endothelial guidance in angiogenic sprouting.** *Organogenesis* 2008;4:241–46 CrossRef Medline
31. Alhusban A, Kozak A, Ergul A, et al. **AT1 receptor antagonism is proangiogenic in the brain: BDNF a novel mediator.** *J Pharmacol Exp Ther* 2013;344:348–59 CrossRef Medline
32. Dvergsten JA, Mueller RG, Griffin P, et al. **Premature cell senescence and T cell receptor-independent activation of CD8+ T cells in juvenile idiopathic arthritis.** *Arthritis Rheum* 2013;65:2201–10 CrossRef Medline
33. Rosset A, Spadola L, Ratib O. **OsiriX: an open-source software for navigating in multidimensional DICOM images.** *J Digit Imaging* 2004;17:205–16 CrossRef Medline
34. Fazekas F, Chawluk JB, Alavi A, et al. **MR signal abnormalities at 1.5 T in Alzheimer's dementia and normal aging.** *AJR Am J Roentgenol* 1987;149:351–56 CrossRef Medline
35. DeCarli C, Fletcher E, Ramey V, et al. **Anatomical mapping of white matter hyperintensities (WMH): exploring the relationships between periventricular WMH, deep WMH, and total WMH burden.** *Stroke* 2005;36:50–55 CrossRef Medline
36. Greenberg SM, Vernooij MW, Cordonnier C, et al; Microbleed Study Group. **Cerebral microbleeds: a guide to detection and interpretation.** *Lancet Neurol* 2009;8:165–74 CrossRef Medline
37. *The SAS System for Windows* [computer progam]. Cary: SAS Institute; 2013
38. *IBM SPSS Statistics for Windows* [computer progam]. Version 22.0. Armonk: IBM; 2013
39. ALZFORUM. AlzGene: Meta-Analysis of All Published AD Association Studies (Case-Control Only) APOE_e2/3/4 2010; http://www.alzgene.org/meta.asp?geneID=83. Accessed September 16, 2016
40. Cheung CY, Ong YT, Ikram MK, et al. **Microvascular network alterations in the retina of patients with Alzheimer's disease.** *Alzheimers Dement* 2014;10:135–42 CrossRef Medline
41. Lai AY, Dorr A, Thomason LA, et al. **Venular degeneration leads to vascular dysfunction in a transgenic model of Alzheimer's disease.** *Brain* 2015;138(pt 4):1046–58 CrossRef Medline
42. Zlokovic BV. **Cerebrovascular effects of apolipoprotein E: implications for Alzheimer disease.** *JAMA Neurol* 2013;70:440–44 CrossRef Medline
43. Brickman AM, Schupf N, Manly JJ, et al. **APOE ε4 and risk for Alzheimer's disease: do regionally distributed white matter hyperintensities play a role?** *Alzheimers Dement* 2014;10:619–29 CrossRef Medline
44. Yates PA, Villemagne VL, Ellis KA, et al. **Cerebral microbleeds: a review of clinical, genetic, and neuroimaging associations.** *Front Neurol* 2014;4:205 CrossRef Medline
45. Hawkes CA, Sullivan PM, Hands S, et al. **Disruption of arterial perivascular drainage of amyloid-beta from the brains of mice expressing the human APOE epsilon4 allele.** *PLoS One* 2012;7:e41636 CrossRef Medline
46. Zipser BD, Johanson CE, Gonzalez L, et al. **Microvascular injury and blood-brain barrier leakage in Alzheimer's disease.** *Neurobiol Aging.* 2007;28:977–86 CrossRef Medline

The authors regret that in the article "In Vivo Imaging of Venous Side Cerebral Small-Vessel Disease in Older Adults: An MRI Method at 7T" (Shaaban CE, Aizenstein HJ, Jorgensen DR, et al. *AJNR Am J Neuroradiol* 2017;38:1923–28; https://doi.org/10.3174/ajnr.A5327), the legend for Fig 1 contained an error. The figure does not contain data used for the analyses. Instead, this is an illustration of the protocol used for tracing. The figure with the corrected legend is reproduced below.

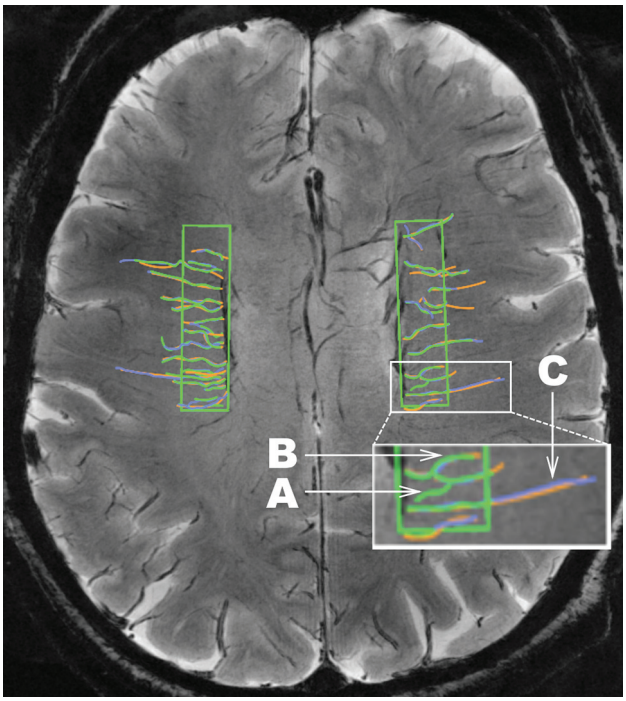

FIG 1. An illustration of the consensus venular tracing method used on SWI at 7T across ROIs in both hemispheres in the LIFE MRI study. Each rater traces the venules. A different color (green, purple, orange) is assigned to each rater, and the 3 sets of tracings are then overlaid. The inset in white is shown at larger magnification at the bottom of the figure to illustrate the following: *A*, Depiction of a venule that would not be included in the dataset because it was traced by only 1 of the 3 raters (green). *B*, An example of a tortuous venule. *C*, An example of a straight venule. Note that this illustration does not represent real data.

http://dx.doi.org/10.3174/ajnr.A5880